

# Synthesis, Structures, and Magnetic Properties of the Copper(II), Cobalt(II), and Manganese(II) Complexes with 9-Acridinecarboxylate and 4-Quinolinecarboxylate Ligands

Xian-He Bu,<sup>\*†</sup> Ming-Liang Tong,<sup>‡</sup> Ya-Bo Xie,<sup>†</sup> Jian-Rong Li,<sup>†</sup> Ho-Chol Chang,<sup>‡</sup> Susumu Kitagawa,<sup>\*,‡</sup> and Joan Ribas<sup>§</sup>

Department of Chemistry, Nankai University, Tianjin 300071, People's Republic of China, Department of Synthetic Chemistry and Biological Chemistry, Graduate School of Engineering, Kyoto University, Kyoto 606-8501, Japan, and Departament de Química Inorgànica, Universitat de Barcelona, Diagonal 647, 08028 Barcelona, Spain

Received June 2, 2005

To explore the relationships between the structures of ligands and their complexes, we have synthesized and characterized a series of metal complexes with two structurally related ligands, 9-acridinecarboxylic acid (HL<sup>1</sup>) and 4-quinolinecarboxylate acid (HL<sup>2</sup>), [Cu<sub>2</sub>(μ<sub>2</sub>-OMe)<sub>2</sub>(L<sup>1</sup>)<sub>2</sub>(H<sub>2</sub>O)<sub>0.69</sub>]<sub>n</sub> **1**, [Cu<sub>2</sub>(L<sup>1</sup>)<sub>4</sub>(CH<sub>3</sub>OH)<sub>2</sub>] **2**, [Cu<sub>3</sub>(L<sup>1</sup>)<sub>6</sub>(CH<sub>3</sub>OH)<sub>6</sub>]·3H<sub>2</sub>O **3**, [Mn<sub>3</sub>(L<sup>1</sup>)<sub>6</sub>(CH<sub>3</sub>OH)<sub>6</sub>]·3H<sub>2</sub>O **4**, [Co<sub>3</sub>(L<sup>1</sup>)<sub>6</sub>(CH<sub>3</sub>OH)<sub>6</sub>]·3H<sub>2</sub>O **5**, [Cu(L<sup>2</sup>)<sub>2</sub>] **6**, [Mn(L<sup>2</sup>)<sub>2</sub>(H<sub>2</sub>O)]<sub>n</sub> **7**, and [Co(L<sup>2</sup>)<sub>2</sub>(H<sub>2</sub>O)]<sub>n</sub> **8**. **1** is a three-dimensional (3D) polymer with an interpenetrating NbO type network showing one-dimensional (1D) channels, whereas **2** and **3** take bi- and trinuclear structures, respectively, because of the differences in basicity of the reaction systems in preparing the three complexes. **4** and **5** have trinuclear structures similar to that of **3**. In **1–5**, ligand L<sup>1</sup> performs different coordination modes with *N,O*-bridging in **1** and *O,O'*-bridging in **2–5**, and the metal ions also show different coordination geometries: square planar in **1**, square pyramidal in **2**, and octahedral in **3–5**. **6** has a two-dimensional structure containing (4,4) grids in which L<sup>2</sup> adopts the *N,O*-bridging mode and the Cu<sup>II</sup> center takes square planar geometry. **7** and **8** are isostructural complexes showing 1D chain structures, with L<sup>2</sup> adopting the *O,O*-bridging mode. In addition, the intermolecular O–H···N hydrogen bonds and π–π stacking interactions further extend the complexes (except **1** and **6**), forming 3D structures. The magnetic properties of **2–7** have been investigated and discussed in detail.

## Introduction

Over the past decades, the construction of metal–organic coordination architectures has witnessed tremendous growth because of their intriguing structures and potential as functional materials.<sup>1–3</sup> Most efforts have been focused on using either neutral ligands (e.g., 4,4'-bipyridine)<sup>4</sup> or anionic

ligands (e.g., carboxylates).<sup>5</sup> However, in recent years, multifunctional ligands bearing both neutral and anionic donor groups have attracted great attention<sup>6</sup> because of their interesting structural features: (1) the presence of different functional groups may allow for diversity in the coordination mode and for the incorporation of interesting properties into the resulting coordination polymers; (2) both neutral and anionic donor groups in such ligands may coordinate to metal centers, resulting in neutral coordination frameworks without

\* To whom correspondence should be addressed. E-mail: buxh@nankai.edu.cn (X.-H.B.), kitagawa@sbchem.kyoto-u.ac.jp (S.K.). Fax: +86-22-23502458 (X.-H.B.), +81-75-7534979 (S.K.).

<sup>†</sup> Nankai University.

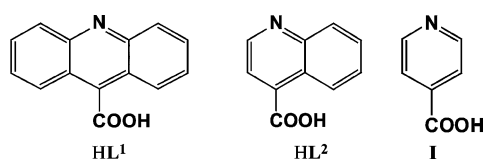
<sup>‡</sup> Kyoto University.

<sup>§</sup> Universitat de Barcelona.

(1) For examples: (a) Braga, D.; Grepioni, F.; Desiraju, G. R. *Chem. Rev.* **1998**, *98*, 1375. (b) Miyasaka, H.; Matsumoto, N.; Okawa, H.; Re, N.; Gallo, E.; Floriani, C. *J. Am. Chem. Soc.* **1996**, *118*, 981. (c) Kobayashi, H.; Tomita, H.; Naito, T.; Kobayashi, A.; Sakai, F.; Watanabe, T.; Cassoux, P. *J. Am. Chem. Soc.* **1996**, *118*, 368. (d) Yaghi, O. M.; Li, H.; Davis, C.; Richardson, D.; Groy, T. L. *Acc. Chem. Res.* **1998**, *31*, 474.

(2) For examples: (a) Yaghi, O. M.; Li, G.; Li, H. *Nature* **1995**, *378*, 703. (b) Sato, O.; Iyoda, T.; Fujishima, A.; Hashimoto, K. *Science* **1996**, *271*, 49. (c) Zaworotko, M. J. *Angew. Chem., Int. Ed.* **2000**, *39*, 3052. (d) Gardner, G. B.; Venkataraman, D.; Moore, J. S.; Lee, S. *Nature* **1995**, *374*, 792. (e) Bu, X. H.; Chen, W.; Lu, S. L.; Zhang, R. H.; Liao, D. Z.; Bu, W. M.; Shionoya, M.; Brisse, F.; Ribas, J. *Angew. Chem., Int. Ed.* **2001**, *40*, 3201. (f) Kou, H. Z.; Gao, S.; Zhang, J.; Wen, G. H.; Su, G.; Zheng, R. K.; Zhang, X. X. *J. Am. Chem. Soc.* **2001**, *123*, 11809.

Chart 1



counterions existing in the cavity or channel, which may possess more empty space than ionic frameworks for entrapping guest molecules.

As typical bifunctional ligands, isonicotinic acid (**I**, see Chart 1) and its derivatives have been widely used to construct metal–organic coordination polymers not only from the viewpoint of structural interest<sup>7</sup> but also for targeting particular solid state complexes with tailored properties such as nonlinear optical properties,<sup>8</sup> inclusion behavior,<sup>9</sup> and molecular magnetism.<sup>10</sup> However, the use of 9-acridinecarboxylic acid (**HL**<sup>1</sup>) and 4-quinolinecarboxylic acid (**HL**<sup>2</sup>)

(Chart 1), two analogues of isonicotinic acid, for the construction of metal–organic frameworks has not been well-documented yet.<sup>11</sup> 9-Acridinecarboxylate and 4-quinolinecarboxylate ligands have several structural characteristics that are different from those of isonicotinate: (1) they have larger conjugated  $\pi$ -systems, and therefore  $\pi$ – $\pi$  stacking interactions may play important roles in the formations of their complexes; (2) the larger systems weaken the coordination abilities of the acridine and quinoline nitrogen atoms; (3) the steric hindrance of benzene rings may affect the coordination abilities of these ligands. These structural characteristics make 9-acridinecarboxylate and 4-quinolinecarboxylate show coordination modes different from those of isonicotinate, and they may form interesting complexes.<sup>11</sup> Herein we report the synthesis, structures, and magnetic properties of some complexes with the two ligands.

## Experimental Section

**Materials and General Methods.** All solvents and starting materials for synthesis were purchased commercially, and were used as received. Elemental analyses were performed on a Yanaco C.H.N. Corder MT-5 or a Perkin-Elmer 240C analyzer. IR spectra were measured on a Hitachi I-5040FT-IR or a TENSOR 27 (Bruker) FT-IR spectrometer with KBr pellets.

**Magnetic Studies.** The variable-temperature magnetic susceptibilities were measured on a Quantum Design SQUID susceptometer operating at a magnetic field of 0.1 T between 2 and 300 K. The diamagnetic corrections were evaluated from Pascal's constants for all the constituent atoms. Magnetization measurements were carried out at low temperature (2 K) in a 0–5 T range.

**Synthesis of Complexes.**  $[\text{Cu}_2(\mu_2\text{-OME})_2(\text{L}^1)_2(\text{H}_2\text{O})_{0.69}]_n$  (**1**),<sup>11a</sup> The MeOH solution of  $\text{Cu}(\text{NO}_3)_2 \cdot 3\text{H}_2\text{O}$  (0.2 mmol, 25 mL) was added to the MeOH solution of **HL**<sup>1</sup> (0.2 mmol, 25 mL) containing an excessive amount of  $\text{Et}_3\text{N}$ . The resulting solution was filtered, and was left to stand at room temperature. Single crystals of **1** suitable for X-ray analysis were obtained after several days.

$[\text{Cu}_2(\text{L}^1)_4(\text{CH}_3\text{OH})_2]$  (**2**). **2** was synthesized by a method similar to that described above except  $\text{Et}_3\text{N}$  was present in a slightly excessive amount. Yield: 50%. Anal. Calcd for  $\text{C}_{58}\text{H}_{40}\text{Cu}_2\text{N}_4\text{O}_{10}$ : C, 64.50; H, 3.73; N, 5.19. Found: C, 64.63; H, 3.64; N, 5.11. IR (KBr pellet,  $\text{cm}^{-1}$ ): 3437w, 1578s, 1434m, 1387s, 1324m, 1290m, 1020m, 764s.

$[\text{Cu}_3(\text{L}^1)_6(\text{CH}_3\text{OH})_6] \cdot 3\text{H}_2\text{O}$  (**3**). To a MeOH/ $\text{CHCl}_3$  solution of **HL**<sup>1</sup> (0.1 mmol) (25 mL) was added a MeOH solution of  $\text{Cu}(\text{NO}_3)_2 \cdot 3\text{H}_2\text{O}$  (0.2 mmol, 25 mL). The resulting solution was filtered, and was left to stand at room temperature. Single crystals of **3** suitable for X-ray analysis were obtained after several days. Yield: 50%. Anal. Calcd for  $\text{C}_{30}\text{H}_{26}\text{Cu}_3\text{N}_2\text{O}_7$ : C, 61.06; H, 4.44; N, 4.75. Found: C, 60.77; H, 4.14; N, 4.78. IR (KBr pellet,  $\text{cm}^{-1}$ ): 3438m, 1584s, 1432m, 1390s, 1321m, 1284m, 767s.

Complexes **4–8** were synthesized by a method similar to that of **3** except **HL**<sup>1</sup> was replaced by **HL**<sup>2</sup> for **6–8**.

$[\text{Mn}_3(\text{L}^1)_6(\text{CH}_3\text{OH})_6] \cdot 3\text{H}_2\text{O}$  (**4**). Yield: 50%. Anal. Calcd for  $\text{C}_{30}\text{H}_{26}\text{Mn}_3\text{N}_2\text{O}_7$ : C, 61.97; H, 4.51; N, 4.82. Found: C, 62.27; H,

- (3) For examples: (a) Blake, A. J.; Champness, N. R.; Hubberstey, P.; Li, W. S.; Withersby, M. A.; Schröder, M. *Coord. Chem. Rev.* **1999**, *183*, 117. (b) Chui, S. S. Y.; Lo, S. M. F.; Charmant, J. P. H.; Orpen, A. G.; Williams, I. D. *Science* **1999**, *283*, 1148. (c) Batten, S. R.; Robson, R. *Angew. Chem., Int. Ed.* **1998**, *37*, 1460. (d) Melcer, N. J.; Enright, G. D.; Ripmeester, J. A.; Shimizu, G. K. H. *Inorg. Chem.* **2001**, *40*, 4641. (e) Fujita, M.; Kwon, Y. J.; Washizu, S.; Ogura, K. *J. Am. Chem. Soc.* **1994**, *116*, 1151. (f) Cao, R.; Sun, D. F.; Liang, Y. C.; Hong, M. C.; Tatsumi, K.; Shi, Q. *Inorg. Chem.* **2002**, *41*, 2087. (g) Tong, M. L.; Wu, Y. M.; Ru, J.; Chen, X. M.; Chang, H. C.; Kitagawa, S. *Inorg. Chem.* **2002**, *41*, 4846. (h) Liu, S. X.; Lin, S.; Lin, B. Z.; Lin, C. C.; Huang, J. Q. *Angew. Chem., Int. Ed.* **2001**, *40*, 1084.
- (4) (a) Robinson, F.; Zaworotko, M. J. *Chem. Commun.* **1995**, 2413. (b) Keller, S. W. *Angew. Chem., Int. Ed.* **1997**, *36*, 247. (c) Gable, R. W.; Hoskins, B. F.; Robson, R. *Chem. Commun.* **1990**, 1677. (d) Hagrman, D.; Zubieta, C.; Rose, D. J.; Zubieta, J.; Haushalter, R. C. *Angew. Chem., Int. Ed.* **1997**, *36*, 873. (e) Lu, J.; Crisci, G.; Niu, T.; Jacobson, A. J. *Inorg. Chem.* **1997**, *36*, 5140. (f) Kondo, M.; Yoshitomi, T.; Seki, K.; Matsuzaka, H.; Kitagawa, S. *Angew. Chem., Int. Ed.* **1997**, *36*, 1725.
- (5) Yaghi, O. M.; Li, H.; Davis, C.; Richardson, D.; Groy, T. L. *Acc. Chem. Res.* **1998**, *31*, 474.
- (6) (a) Homanen, P.; Haukka, M.; Ahlgrén, M.; Pakkanen, T. A. *Inorg. Chem.* **1997**, *36*, 3794. (b) Eskelinen, E.; Luukkanen, S.; Haukka, M.; Ahlgrén, M.; Pakkanen, T. A. *J. Chem. Soc., Dalton Trans.* **2000**, 2745. (c) Moghimi, A.; Alizadeh, R.; Shokrollahi, A.; Aghabozorg, H.; Shamsipur, M.; Shokravi, A. *Inorg. Chem.* **2003**, *42*, 1616. (d) Zhang, X. M.; Tong, M. L.; Chen, X. M. *Angew. Chem., Int. Ed.* **2002**, *41*, 1029. (e) Zhang, X. M.; Tong, M. L.; Gong, M. L.; Lee, H. K.; Luo, L.; Li, K. F.; Tong, Y. X.; Chen, X. M. *Chem.–Eur. J.* **2002**, *8*, 3187. (f) Zheng, S. L.; Zhang, J. P.; Wong, W. T.; Chen, X. M. *J. Am. Chem. Soc.* **2003**, *125*, 6882. (g) Xiong, R. G.; You, X. Z.; Abrahams, B. F.; Xue, Z.; Che, C. M. *Angew. Chem., Int. Ed.* **2001**, *40*, 4422.
- (7) (a) Xiong, R. G.; Zuo, J. L.; You, X. Z.; Fun, H. K.; Raj, S. S. S. *New J. Chem.* **1999**, *23*, 1051. (b) Min, K. S.; Suh, M. P. *Eur. J. Inorg. Chem.* **2001**, 449. (c) Evans, O. R.; Wang, Z. Y.; Xiong, R. G.; Foxman, B. M.; Lin, W. B. *Inorg. Chem.* **1999**, *38*, 2969. (d) Evans, O. R.; Lin, W. B. *Inorg. Chem.* **2000**, *39*, 2189. (e) Zheng, S. L.; Tong, M. L.; Yu, X. L.; Chen, X. M. *J. Chem. Soc., Dalton Trans.* **2001**, 586. (f) Xiong, R. G.; Wilson, S. R.; Lin, W. B. *J. Chem. Soc., Dalton Trans.* **1998**, 4089. (g) Evans, O. R.; Xiong, R. G.; Wang, Z. Y.; Wong, G. K.; Lin, W. B. *Angew. Chem., Int. Ed.* **1999**, *38*, 536. (h) Lu, J. Y.; Babb, A. M. *Chem. Commun.* **2001**, 821.
- (8) (a) Evans, O. R.; Lin, W. B. *Acc. Chem. Res.* **2002**, *35*, 511. (b) Lin, W. B.; Evans, O. R.; Xiong, R. G.; Wang, Z. Y. *J. Am. Chem. Soc.* **1998**, *120*, 13273. (c) Lin, W. B.; Ma, L.; Evans, O. R. *Chem. Commun.* **2000**, 2263.
- (9) (a) Aakeröy, C. B.; Beatty, A. M.; Leinen, D. S. *Angew. Chem., Int. Ed.* **1999**, *38*, 1815. (b) Sekiya, R.; Nishikiori, S.-I. *Chem.–Eur. J.* **2000**, *8*, 4803. (c) Zhang, J.; Lin, W. B.; Chen, Z. F.; Xiong, R. G.; Abrahams, B. F.; Fun, H. K. *J. Chem. Soc., Dalton Trans.* **2001**, 1806.
- (10) Chapman, M. E.; Ayyappan, P.; Foxman, B. M.; Yee, G. T.; Lin, W. B. *Cryst. Growth Des.* **2001**, *1*, 159.

- (11) (a) Bu, X.-H.; Tong, M.-L.; Chang, H.-C.; Kitagawa, S.; Batten, S. R. *Angew. Chem., Int. Ed.* **2004**, *43*, 192. (b) Xiong, R. G.; Zuo, J. L.; You, X. Z.; Fun, H. K.; Raj, S. S. S. *Organometallics* **2000**, *19*, 1183. (c) Chen, Z. F.; Zhang, P.; Xiong, R. G.; Liu, D. J.; You, X. Z. *Inorg. Chem. Commun.* **2002**, *5*, 35. (d) Bu, X.-H.; Tong, M.-L.; Li, J.-R.; Chang, H.-C.; Li, L.-J.; Kitagawa, S. *CrystEngComm* **2005**, *7*, 411.

**Table 1.** Crystallographic Data and Structure Refinement Summary for 2–8

	2	3	4	5
chemical formula	C <sub>58</sub> H <sub>40</sub> Cu <sub>2</sub> N <sub>4</sub> O <sub>10</sub>	C <sub>90</sub> H <sub>78</sub> Cu <sub>3</sub> N <sub>6</sub> O <sub>21</sub>	C <sub>90</sub> H <sub>78</sub> Mn <sub>3</sub> N <sub>6</sub> O <sub>21</sub>	C <sub>90</sub> H <sub>78</sub> Co <sub>3</sub> N <sub>6</sub> O <sub>21</sub>
fw	1080.02	1770.25	1744.40	1756.37
space group	<i>P</i> $\bar{1}$	<i>Pa</i> -3	<i>Pa</i> -3	<i>Pa</i> -3
<i>a</i> (Å)	10.060(8)	19.990(2)	20.205(2)	20.007(3)
<i>b</i> (Å)	10.676(8)	19.990(2)	20.205(2)	20.007(3)
<i>c</i> (Å)	11.79(1)	19.990(2)	20.205(2)	20.007(3)
$\alpha$ (deg)	90.987(8)	90	90	90
$\beta$ (deg)	110.29(1)	90	90	90
$\gamma$ (deg)	94.560(9)	90	90	90
<i>V</i> (Å <sup>3</sup> )	1183(2)	7988(1)	8248(2)	8008(2)
<i>Z</i>	1	4	4	4
<i>D</i> (g cm <sup>-3</sup> )	1.516	1.427	1.405	1.457
$\mu$ (mm <sup>-1</sup> )	0.968	0.872	0.531	0.695
<i>T</i> (K)	293(2)	293(2)	293(2)	293(2)
<i>R</i> <sup>a</sup> / <i>wR</i> <sup>b</sup>	0.0497/0.1333	0.1240/0.2292	0.0559/0.1390	0.0492/0.1289

	6	7	8
chemical formula	C <sub>20</sub> H <sub>12</sub> CuN <sub>2</sub> O <sub>4</sub>	C <sub>20</sub> H <sub>14</sub> MnN <sub>2</sub> O <sub>5</sub>	C <sub>20</sub> H <sub>14</sub> CoN <sub>2</sub> O <sub>5</sub>
fw	407.86	417.27	421.26
space group	<i>C2/c</i>	<i>C2/c</i>	<i>C2/c</i>
<i>a</i> (Å)	13.61(3)	15.08(5)	14.926(5)
<i>b</i> (Å)	10.90(2)	14.39(3)	14.42(2)
<i>c</i> (Å)	13.23(3)	7.71(2)	7.529(3)
$\alpha$ (deg)	90	90	90
$\beta$ (deg)	117.39(4)	92.4(1)	92.33(3)
$\gamma$ (deg)	90	90	90
<i>V</i> (Å <sup>3</sup> )	1741(7)	1671(8)	1619(3)
<i>Z</i>	4	4	4
<i>D</i> (g cm <sup>-3</sup> )	1.556	1.659	1.728
$\mu$ (mm <sup>-1</sup> )	1.284	0.828	1.099
<i>T</i> (K)	293(2)	293(2)	293(2)
<i>R</i> <sup>a</sup> / <i>wR</i> <sup>b</sup>	0.0336/0.0817	0.0604/0.1620	0.0392/0.1068

$$^a R = \sum(|F_o| - |F_c|) / \sum|F_o|. \quad ^b wR = [\sum w(|F_o|^2 - |F_c|^2)^2 / \sum w(F_o^2)]^{1/2}.$$

4.90; N, 4.69. IR (KBr pellet, cm<sup>-1</sup>): 3446m, 1590vs, 1445m, 1395s, 1328m, 1027m, 763s.

[Co<sub>3</sub>(L<sup>1</sup>)<sub>6</sub>(CH<sub>3</sub>OH)<sub>6</sub>·3H<sub>2</sub>O (5). Yield: 40%. Anal. Calcd for C<sub>30</sub>H<sub>26</sub>CoN<sub>2</sub>O<sub>7</sub>: C, 61.54; H, 4.48; N, 4.78. Found: C, 61.98; H, 4.94; N, 4.57. IR (KBr pellet, cm<sup>-1</sup>): 3441m, 1591vs, 1458m, 1400s, 1320m, 767s, 653m.

[Cu(L<sup>2</sup>)<sub>2</sub>]<sub>n</sub> (6). Yield: 45%. Anal. Calcd for C<sub>20</sub>H<sub>12</sub>CuN<sub>2</sub>O<sub>4</sub>: C, 58.90; H, 2.97; N, 6.87. Found: C, 58.86; H, 2.93; N, 6.75. IR (KBr pellet, cm<sup>-1</sup>): 3437m, 1618s, 1574m, 1514m, 1355vs, 1298m, 776m, 696m.

[Mn(L<sup>2</sup>)<sub>2</sub>(H<sub>2</sub>O)]<sub>n</sub> (7). Yield: 50%. Anal. Calcd for C<sub>20</sub>H<sub>14</sub>MnN<sub>2</sub>O<sub>5</sub>: C, 57.57; H, 3.38; N, 6.71. Found: C, 57.16; H, 3.48; N, 6.56. IR (KBr pellet, cm<sup>-1</sup>): 3441m, 1583s, 1462m, 1394s, 1304w, 766s.

[Co(L<sup>2</sup>)<sub>2</sub>(H<sub>2</sub>O)]<sub>n</sub> (8). Yield: 45%. Anal. Calcd for C<sub>20</sub>H<sub>14</sub>CoN<sub>2</sub>O<sub>5</sub>: C, 57.02; H, 3.35; N, 6.65. Found: C, 56.97; H, 3.44; N, 6.61. IR (KBr pellet, cm<sup>-1</sup>): 3460m, 1603s, 1509m, 1408s, 1304w, 766s, 654m.

**X-ray Crystallography.** Details of crystallographic parameters, data collection, and refinements are summarized in Table 1. Intensity data were collected on a Rigaku/MSC Mercury CCD diffractometer with graphite-monochromated Mo K $\alpha$  radiation ( $\lambda$  = 0.71069 Å) at 293 (±2) K. The structures were solved by direct methods, and were refined anisotropically by the full-matrix least-squares technique using the SHELX 97 program package. The coordinates of the non-hydrogen atoms were refined anisotropically, whereas non-water hydrogen atoms were included in the calculated positions and refined with isotropic thermal parameters riding on the parent atoms. The H atoms of water molecules were fixed by difference Fourier *E*-maps. Selected bond lengths and angles for 2–8 are listed in Table 2.

## Results and Discussions

**Syntheses and General Characterizations.** HL<sup>I</sup> is slightly soluble in MeOH, but becomes soluble with the addition of Et<sub>3</sub>N. Three Cu<sup>II</sup> complexes of L<sup>I</sup> taking different structures 1–3 could be isolated under different basicities. In the preparation for 1, the basicity should be high enough so that methanol is deprotonated to coordinate to Cu<sup>II</sup>.<sup>11a</sup> The structural differences of 2 and 3 are also due to the differences of basicity in the reaction systems. Other metal ions are not so sensitive to the basicities of the reaction systems, and only one kind of complex (4 and 5, and 7 and 8) was obtained. In addition, two kinds of Cu<sup>II</sup> complexes with L<sup>2</sup> (6) were obtained, one green and the other blue, but the green one is not stable, and has not been characterized.

One feature of the IR data is the separation between  $\nu_{as}(\text{COO}^-)$  and  $\nu_s(\text{COO}^-)$ , which have often been used to diagnose the coordination modes in the carboxylate ligands.<sup>12</sup> The separation for monodentate carboxylate groups is >200 cm<sup>-1</sup>, whereas it is <200 cm<sup>-1</sup> in bidentate groups.<sup>12,13</sup> The separation ( $\Delta$ ) between  $\nu_{as}(\text{COO}^-)$  and  $\nu_s(\text{COO}^-)$  is 229 cm<sup>-1</sup> for 1 and 263 cm<sup>-1</sup> for 6, indicating a monodentate coordination mode for coordinated carboxylate groups. The  $\Delta$  values for other complexes are 191 cm<sup>-1</sup> for 2, 196 cm<sup>-1</sup> for 3, 195 cm<sup>-1</sup> for 4, 191 cm<sup>-1</sup> for 5, 189 cm<sup>-1</sup> for 7, and 195 cm<sup>-1</sup> for 8, indicating bidentate coordinating modes for

(12) Deacon, G. B.; Phillips, R. J. *Coord. Chem. Rev.* **1980**, *33*, 227.

(13) Nakamoto, K. *Infrared and Raman Spectra of Inorganic and Coordination Compounds*; John Wiley & Sons: New York, 1986.

**Table 2.** Selected Bond Lengths (Å) and Angles (deg) for Complexes 2–8

[Cu <sub>2</sub> (L <sup>1</sup> ) <sub>4</sub> (CH <sub>3</sub> OH) <sub>2</sub> ] (2) <sup>a</sup>			
Cu(1)–O(4) <sup>i</sup>	1.964(3)	Cu(1)–O(3)	1.964(3)
Cu(1)–O(1)	1.973(3)	Cu(1)–O(5)	2.147(3)
O(4) <sup>i</sup> –Cu(1)–O(2) <sup>i</sup>	92.8(1)	O(2) <sup>i</sup> –Cu(1)–O(3)	87.8(1)
O(4) <sup>i</sup> –Cu(1)–O(1)	87.7(1)	O(3)–Cu(1)–O(1)	89.2(1)
O(2) <sup>i</sup> –Cu(1)–O(5)	98.6(1)	O(3)–Cu(1)–O(5)	89.8(1)
[Cu <sub>3</sub> (L <sup>1</sup> ) <sub>6</sub> (CH <sub>3</sub> OH) <sub>6</sub> ]·3H <sub>2</sub> O (3) <sup>b</sup>			
Cu(1)–O(1)	2.033(6)	Cu(1)–O(3)	2.112(7)
Cu(2)–O(2)	2.068(6)		
O(1) <sup>i</sup> –Cu(1)–O(1)	100.9(2)	O(1) <sup>i</sup> –Cu(1)–O(3)	89.4(3)
O(1)–Cu(1)–O(3)	84.8(3)	O(1) <sup>ii</sup> –Cu(1)–O(3)	167.0(3)
O(3) <sup>ii</sup> –Cu(1)–O(3)	83.6(2)	O(2) <sup>i</sup> –Cu(2)–O(2)	93.1(3)
O(2) <sup>iii</sup> –Cu(2)–O(2)	86.9(3)		
[Mn <sub>3</sub> (L <sup>1</sup> ) <sub>6</sub> (CH <sub>3</sub> OH) <sub>6</sub> ]·3H <sub>2</sub> O (4) <sup>c</sup>			
Mn(1)–O(1)	2.126(2)	Mn(1)–O(3)	2.224(2)
Mn(2)–O(2)	2.155(2)		
O(1)–Mn(1)–O(1) <sup>i</sup>	101.07(7)	O(1)–Mn(1)–O(3) <sup>ii</sup>	88.70(8)
O(1)–Mn(1)–O(3)	84.77(8)	O(3) <sup>ii</sup> –Mn(1)–O(3)	84.10(9)
O(2) <sup>j</sup> –Mn(2)–O(2)	92.30(8)	O(2) <sup>ii</sup> –Mn(2)–O(2) <sup>i</sup>	87.09(8)
O(1) <sup>ii</sup> –Mn(1)–O(3)	167.31(8)		
[Co <sub>3</sub> (L <sup>1</sup> ) <sub>6</sub> (CH <sub>3</sub> OH) <sub>6</sub> ]·3H <sub>2</sub> O (5) <sup>d</sup>			
Co(1)–O(1)	2.057(2)	Co(1)–O(3)	2.131(2)
Co(2)–O(2)	2.083(2)		
O(1) <sup>j</sup> –Co(1)–O(1)	99.67(7)	O(1)–Co(1)–O(3) <sup>ii</sup>	89.81(8)
O(1)–Co(1)–O(3)	85.26(8)	O(3)–Co(1)–O(3) <sup>ii</sup>	84.20(8)
O(2) <sup>i</sup> –Co(2)–O(2)	92.91(8)	O(2) <sup>iii</sup> –Mn(2)–O(2) <sup>i</sup>	87.70(8)
O(1) <sup>ii</sup> –Mn(1)–O(3)	168.34(8)		
[Cu(L <sup>2</sup> ) <sub>2</sub> ] <sub>n</sub> (6) <sup>e</sup>			
Cu(1)–O(1)	1.937(3)	Cu(1)–N(1) <sup>ii</sup>	1.999(3)
O(1) <sup>j</sup> –Cu(1)–O(1)	91.2(2)	O(1)–Cu(1)–N(1) <sup>ii</sup>	88.9(2)
O(1) <sup>j</sup> –Cu(1)–N(1) <sup>ii</sup>	174.34(9)		
[Mn(L <sup>2</sup> ) <sub>2</sub> (H <sub>2</sub> O)] <sub>∞</sub> (7) <sup>f</sup>			
Mn(1)–O(2) <sup>i</sup>	2.094(6)	Mn(1)–O(1)	2.175(5)
Mn(1)–O(1W)	2.307(5)		
O(2) <sup>j</sup> –Mn(1)–O(1)	88.0(3)	O(2) <sup>ii</sup> –Mn(1)–O(1)	92.0(3)
O(1) <sup>iii</sup> –Mn(1)–O(1W)	89.0(2)	O(2) <sup>j</sup> –Mn(1)–O(1W)	91.6(2)
O(2) <sup>ii</sup> –Mn(1)–O(1W)	88.4(2)	O(1)–Mn(1)–O(1W)	90.7(2)
[Co(L <sup>2</sup> ) <sub>2</sub> (H <sub>2</sub> O)] <sub>∞</sub> (8) <sup>g</sup>			
Co(1)–O(2) <sup>i</sup>	2.021(2)	Co(1)–O(1)	2.091(3)
Co(1)–O(1W)	2.235(2)		
O(2) <sup>j</sup> –Co(1)–O(1)	91.7(1)	O(2) <sup>ii</sup> –Co(1)–O(1)	88.3(1)
O(2) <sup>j</sup> –Co(1)–O(1W)	88.9(1)	O(2) <sup>ii</sup> –Co(1)–O(1W)	91.1(1)

<sup>a</sup> Symmetry code for **2**:  $i = -x, -y, -z + 1$ . <sup>b</sup> Symmetry codes for **3**:  $i = z, x, y$ ;  $ii = y, z, x$ ;  $iii = -y, -z, -x$ . <sup>c</sup> Symmetry codes for **4**:  $i = y - 1/2, -z + 3/2, -x + 1$ ;  $ii = -z + 1, x + 1/2, -y + 3/2$ ;  $iii = z - 1, -x + 1/2, y + 1/2$ . <sup>d</sup> Symmetry codes for **5**:  $i = y - 1/2, -z + 3/2, -x + 1$ ;  $ii = -y + 1/2, z - 1/2, x + 1$ ;  $iii = z - 1, -x + 1/2, y + 1/2$ . <sup>e</sup> Symmetry codes for **6**:  $i = -x + 1, y, -z + 1/2$ ;  $ii = x + 1/2, y - 1/2, z$ . <sup>f</sup> Symmetry codes for **7**:  $i = x, -y, z - 1/2$ ;  $ii = -x, y, -z + 1/2$ ;  $iii = -x, -y, -z$ . <sup>g</sup> Symmetry codes for **8**:  $i = -x, y, -z + 1/2$ ;  $ii = x, -y, z - 1/2$ ;  $iii = -x, -y, -z$ .

the coordinated carboxylate groups. These IR results are coincident with the crystallographic structural analyses. The elemental analysis results of these complexes further confirmed their chemical formulas.

**Descriptions of Crystal Structures. Three-Dimensional Complex [Cu<sub>2</sub>(μ<sub>2</sub>-Ome)<sub>2</sub>(L<sup>1</sup>)<sub>2</sub>·(H<sub>2</sub>O)<sub>0.69</sub>]<sub>n</sub> (1).** Complex **1** is a three-dimensional (3D) neutral framework with a 2-fold interpenetrating NbO type topology consisting of Cu<sub>2</sub>(μ<sub>2</sub>-Ome)<sub>2</sub> dimers bridged by two connecting L<sup>1</sup> ligands.<sup>11a</sup> In **1**, L<sup>1</sup> shows an *N,O*-bridging mode, and the Cu<sup>II</sup> ion adopts square planar coordination geometry. The formation of the Cu<sub>2</sub>(μ<sub>2</sub>-Ome)<sub>2</sub> dimer is the key to forming the 3D structure. In addition, intra- and internetwork CH⋯π and π–π interactions were observed, which may help stabilize the adopted structure.

**Dinuclear Complex [Cu<sub>2</sub>(L<sup>1</sup>)<sub>4</sub>(CH<sub>3</sub>OH)<sub>2</sub>] (2) and Trinuclear Isostructural Complexes [Cu<sub>3</sub>(L<sup>1</sup>)<sub>6</sub>(CH<sub>3</sub>OH)<sub>6</sub>]·3H<sub>2</sub>O (3), [Mn<sub>3</sub>(L<sup>1</sup>)<sub>6</sub>(CH<sub>3</sub>OH)<sub>6</sub>]·3H<sub>2</sub>O (4), and [Co<sub>3</sub>(L<sup>1</sup>)<sub>6</sub>(CH<sub>3</sub>OH)<sub>6</sub>]·3H<sub>2</sub>O (5).** The structure of **2** consists of a centrosymmetric wheel-shaped dinuclear neutral molecule [Cu(L<sup>2</sup>)<sub>2</sub>(MeOH)]<sub>2</sub> (Figure 1). In the dinuclear unit, there are two crystallographically identical Cu<sup>II</sup> centers bridged by four carboxylate groups of four distinct L<sup>1</sup> ligands. Each Cu<sup>II</sup> center is pentacoordinated to four oxygen atoms of the carboxylate groups from different ligands (average Cu–O length: 1.966 Å) in the equatorial plane and one oxygen atom of the MeOH molecule at the axial position. As expected, the axial Cu–O distance of 2.147(3) Å (Cu(1)–O(5)) is significantly longer than that of those in the equatorial plane. In the equatorial position, the Cu(1)–O(1) distance is a little longer than the other three Cu–O bonds, probably because of the steric hindrance of the coordinated MeOH. Several parameters are used to define the coordination geometry of the pentacoordinated metal center, and one of the most common parameters is the τ factor, defined by Addison et al.<sup>14</sup> The τ value is 0.006 for Cu<sup>II</sup> in **2**, indicating

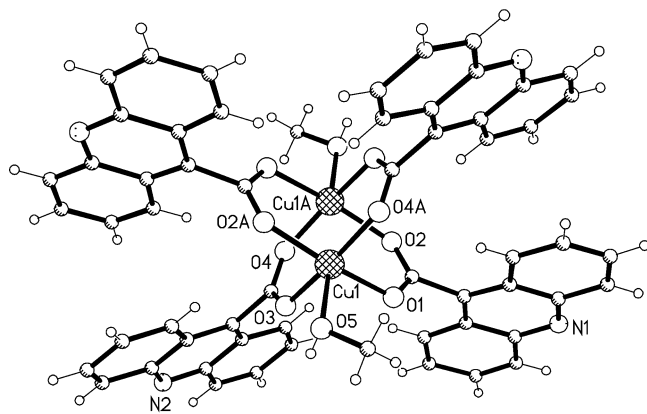
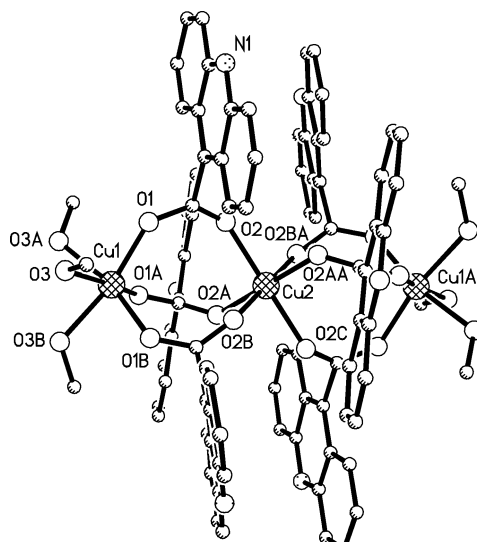


Figure 1. View of the binuclear structure of **2**.

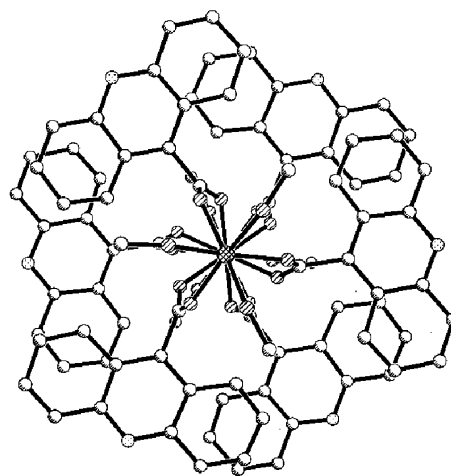
an almost-ideal square pyramidal coordination environment, and the Cu<sup>II</sup> ion deviates from the mean equatorial plane of the square pyramid toward the apical O(5) atom by ca. 0.2051 Å. The bond angles around the Cu<sup>II</sup> center deviate only slightly from 90 or 180°. Interestingly, the Cu–Cu distance of 2.649(2) Å in the dinuclear unit is well below the summed van der Waals radii of two Cu atoms (2.8 Å) but is slightly longer than the Cu–Cu separation of 2.56 Å in metallic copper.<sup>15</sup>

Ligand **L**<sup>1</sup> in **2** adopts a bidentate bridging coordination mode using two oxygen atoms of the carboxylate group with the nitrogen atom remaining uncoordinated. The dihedral angle between the carboxylate plane and the acridine group is 80.8°. The planes of acridine groups in the symmetry position are parallel to each other, whereas the neighboring acridine rings are inclined to each other with the dihedral angle of 31.3°. It should be noted that a 1D structure along the *b* direction is formed through intermolecular O–H⋯N hydrogen bonding interactions. Each N(2) atom of the acridine group serves as an acceptor to form O(5)–H(5)⋯N(2) intermolecular hydrogen bonds with the coordinated MeOH molecules (Figure S1a). The O⋯N distance of 2.785(5) Å and the O–H⋯N angle of 174(5)° fall into the normal range of hydrogen bond interactions. In addition, the adjacent acridine rings from different dinuclear units are aligned in an offset fashion, and are approximately parallel to each other with a center–center distance of ca. 3.6 Å, indicating the presence of face-to-face  $\pi$ – $\pi$  stacking interactions (Figure S1b). The co-effects of hydrogen bonding and  $\pi$ – $\pi$  stacking interactions stabilize this 1D structure.

Complexes **3**, **4**, and **5** are isostructural neutral molecules with trinuclear structures, and also have the same packing modes.<sup>11d</sup> Here we describe only **3** in detail. Related structural parameters of the other two complexes are listed in Table 2. The structure of **3** consists of a centrosymmetric trinuclear double-wheel molecule [Cu<sub>3</sub>(L<sup>1</sup>)<sub>6</sub>(MeOH)<sub>6</sub>] and uncoordinated water molecules. In the trinuclear unit, there are two crystallographically independent Cu<sup>II</sup> centers, with Cu(2) being located at the inversion center (Figure 2). The Cu(2)



(a)



(b)

Figure 2. Trinuclear structure of **3**. (a) Side view. (b) Top view.

ion is coordinated to six carboxylate oxygen atoms from six different acridinecarboxylate ligands. The six Cu(2)–O bond lengths are equal, and the bond angles around the Cu(2) center (86.9(3) or 93.1(3)°) are close to 90°, showing almost-ideal octahedral geometry. Cu(1) is also six-coordinated to six oxygen atoms: three from three distinct acridinecarboxylate ligands with equal Cu–O bond distances (2.033–(6) Å), and the other three from three methanol molecules (Cu–O bond length is 2.112(7) Å). The geometry around the Cu(1) center can be described as a slightly distorted octahedron.

In the trinuclear unit, all acridinecarboxylate ligands adopt an *O,O*-bidentate bridging coordination mode using carboxylate groups to coordinate to Cu<sup>II</sup> centers with an adjacent Cu⋯Cu distance of 4.227 Å. In each acridinecarboxylate ligand, the mean plane of the carboxylate group and the plane of the acridine group are almost perpendicular to each other, with a dihedral angle of 84.7°. Adjacent acridine rings in the same wheel are inclined to each other at an angle of 17.1°, reducing steric hindrance. The two planes of the acridine rings at the symmetric site are parallel to each other. In the axial direction, the center–center distance of adjacent

(14) Addison, A. W.; Rao, T. N.; Reedijk, J.; van Rijn, J.; Verschoor, G. C. *J. Chem. Soc., Dalton Trans.* **1984**, 1349.

(15) Jones, P. L.; Jeffery, J. C.; Maher, J. P.; McCleverty, J. A.; Rieger, P. H.; Ward, M. D. *Inorg. Chem.* **1997**, *36*, 3088.

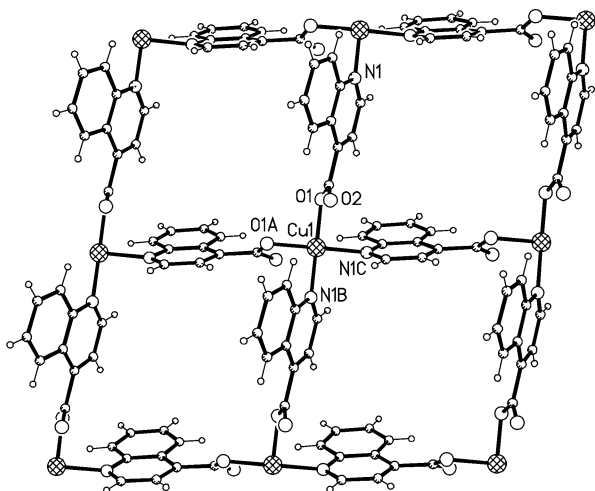


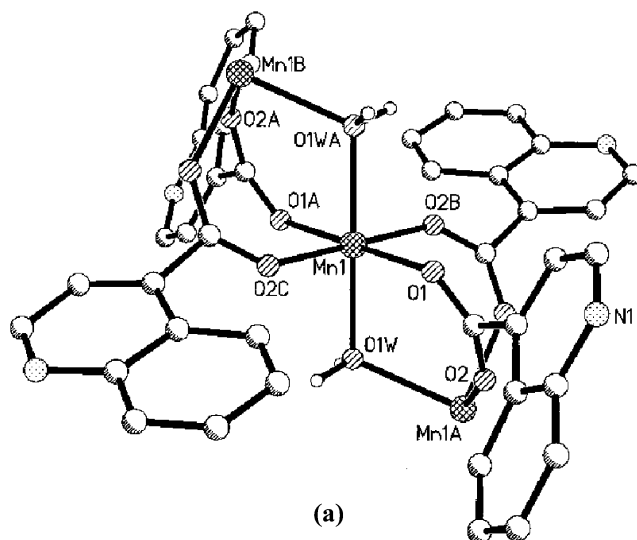
**Figure 3.** View of the 2D grid structure of **6**.

aromatic rings is only 3.524 Å, indicating significant intramolecular  $\pi$ - $\pi$  stacking interactions, which may help form and stabilize the trinuclear structure.

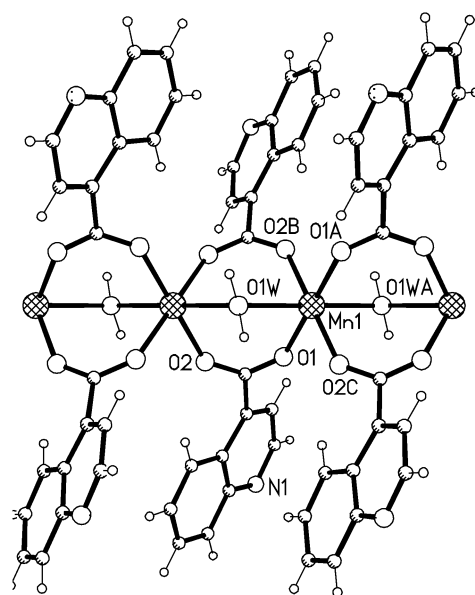
It should be noted that the acridine nitrogen atoms from a trinuclear unit accept the hydrogen atoms from coordinated methanol molecules of adjacent trinuclear units to form intermolecular O-H $\cdots$ N hydrogen bonds with an O $\cdots$ N distance of 2.789(6) Å and an O-H $\cdots$ N bond angle of 166-(7)° (Figure S2a), resulting in a 3D topology (Figure S2b), and these hydrogen bonds further stabilize the structure.

**2D Complex [Cu(L<sup>2</sup>)<sub>2</sub>]<sub>n</sub> (6).** Complex **6** is an infinite square-grid structure consisting of four-coordinate Cu<sup>II</sup> centers and 4-quinolinecarboxylate bridging groups (Figure 3). The asymmetric unit contains a Cu<sup>II</sup> center and two *N,O*-bidentate 4-quinolinecarboxylate bridging groups. The Cu<sup>II</sup> center lies on a crystallographic 2-fold axis, and is coordinated to two quinoline nitrogen atoms and two carboxylate oxygen atoms from four different 4-quinolinecarboxylate ligands in a *syn* configuration. The Cu-O and Cu-N bond distances are 1.937(3) and 1.999(3) Å, respectively, which are in the normal range for such complexes.<sup>7g,10</sup> The *cis* bond angles around the Cu<sup>II</sup> center are 88.9(2) and 91.7(2)°. The Cu<sup>II</sup> center is almost in the plane formed by four coordination donors, and the geometry around it can be described as slightly distorted square planar.

Each Cu<sup>II</sup> center is linked to four adjacent Cu<sup>II</sup> centers by four *exo* bidentate ligands, resulting in a 2D neutral rhombohedral grid in the *ab* plane with a (4,4) topology. The shorter and longer diagonals of the rhombohedral grid run along the *b* and *a* axes, respectively. The 4-quinolinecarboxylate ligands behave as rigid linear linkers, with a dihedral angle of 32.0° between the carboxylate plane and the quinoline group. At first glance, there seems to be empty space in **6**, with a Cu-Cu separation of 8.715 Å. A closer examination reveals that the quinoline rings of 4-quinolinecarboxylate groups partially intrude into the rhombohedral cavities, resulting in interdigitation of the rhombohedral networks (Figure S3). The interdigitated quinoline rings are parallel to each other, with an interplanar distance of 4.766 Å. The interdigitation of quinoline rings from adjacent



(a)



(b)

**Figure 4.** (a) Coordination environment of the Mn<sup>II</sup> center in **7**. (b) The 1D chain structure.

rhombohedral grids has efficiently filled in all the empty space; therefore, no solvent molecules are enclathrated in **6**.

**Two 1D Chain Complexes [Mn(L<sup>2</sup>)<sub>2</sub>(H<sub>2</sub>O)]<sub>n</sub> (7) and [Co(L<sup>2</sup>)<sub>2</sub>(H<sub>2</sub>O)]<sub>n</sub> (8).** Complexes **7** and **8** are isostructural, and we describe only **7** in detail here. The asymmetric unit of **7** consists of a Mn<sup>II</sup> ion, two 4-quinolinecarboxylate groups, and a water molecule. The geometry around the Mn<sup>II</sup> center can be best described as a slightly distorted octahedron (Figure 4a). Each Mn<sup>II</sup> ion is coordinated to four carboxylate oxygen atoms from four different 4-quinolinecarboxylate groups in the equatorial plane and two oxygen atoms from two H<sub>2</sub>O molecules at the axial position, and these coordinated oxygen atoms are related by an inversion center lying at the Mn<sup>II</sup> ion. All the Mn-O bond distances are normal. In the equatorial plane, the bond distance of Mn(1)-O(1) (2.175(5) Å) is slightly longer than that of Mn(1)-O(2) (2.094(6) Å), and the bond length of Mn-O at the axial position is 2.307(5) Å. The bond angles around Mn<sup>II</sup> range

from 88.4(2) to 92.0(3)°, deviating less than 2° from an ideal octahedral geometry.

In **7**, each 4-quinolinecarboxylate adopts an *O,O*-bidentate bridging mode using a carboxylate group with the quinoline nitrogen noncoordinated. Adjacent Mn<sup>II</sup> centers are doubly bridged by the 4-quinolinecarboxylate ligands, forming an infinite chain along the *c* direction, with a Mn–Mn distance of 3.855 Å (Figure 4b). Two carboxylate groups bridge two adjacent Mn<sup>II</sup> centers to form an eight-membered ring. Furthermore, the coordinated water molecules bridge Mn<sup>II</sup> centers to complete the octahedral geometry of Mn<sup>II</sup> ions. In each 4-quinolinecarboxylate ligand, the mean plane of the carboxylate group and the plane of the quinoline group are inclined to each other with a dihedral angle of 49.2°. The two planes of quinoline rings at the symmetric places are parallel to each other, whereas the two adjacent quinoline rings are inclined to each other with a dihedral angle of 54.4°.

Another feature of **7** resides in the formation of a 3D structure through hydrogen bonds between coordinated H<sub>2</sub>O and quinoline N (O⋯N = 2.750 Å). Each water molecule links two quinoline nitrogens of different chains through intermolecular O–H⋯N linkages, and each chain links four adjacent chains through the hydrogen bonds to form a 3D structure (Figure S4) in which the rhombic channels formed by four adjacent chains are occupied by quinoline rings. In the *ab* plane, the adjacent Mn⋯Mn nonbonding distances are 10.42 and 11.10 Å. In addition, the separation of the parallel aromatic rings along the *c* direction is 3.70 Å, indicating the presence of intermolecular face-to-face  $\pi$ – $\pi$  stacking interactions. The co-effects of H-bonding and  $\pi$ – $\pi$  stacking interactions further stabilize this 3D network.

As expected, Mn<sup>II</sup> and Co<sup>II</sup> show octahedral coordination geometries in all related complexes, whereas the Cu<sup>II</sup> ion adopts square planar, square pyramidal, and octahedral coordination geometries in complexes **1**–**3**, respectively. The flexibility of the coordination geometry of Cu<sup>II</sup> provides the possibility of adjusting the structures of its complexes by varying the reaction conditions. Because of the differences in basicity in the reaction systems, complexes **1**–**3** take different structures with different coordination modes of ligand **L**<sup>1</sup> and different geometries of the Cu<sup>II</sup> ions.

This work gives a good comparison to the analogous isonicotinate (**I**) complexes, in which the pyridine nitrogen generally acts as a donor to coordinate to the metal ion in five- and six-coordinate complexes.<sup>7–10</sup> However, in the 4-quinolinecarboxylate and 9-acridinecarboxylate complexes described here, the quinoline and acridine nitrogens are uncoordinated to metal centers except in **1** and **6**, in which the metal centers are four-coordinated. This is probably attributable to the steric hindrance of the side benzene rings, which may obstruct the coordination of the nitrogen atom. Although the nitrogen atoms in ligands **2**–**5**, **7**, and **8** are noncoordinated, they act as H acceptors for forming intermolecular O–H⋯N H-bonds with coordinated MeOH molecules or H<sub>2</sub>O. The intermolecular O–H⋯N H-bonds not only link these discrete or 1D molecules into high-dimensional structures but also play important roles in stabilizing these complexes. In addition, the large conjugated

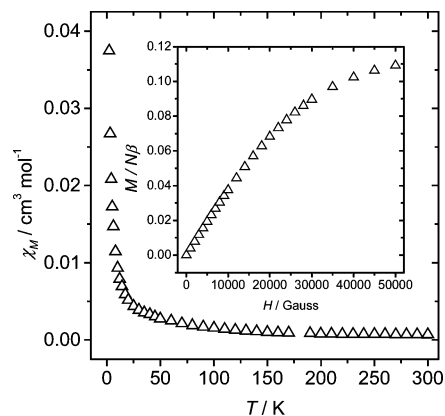
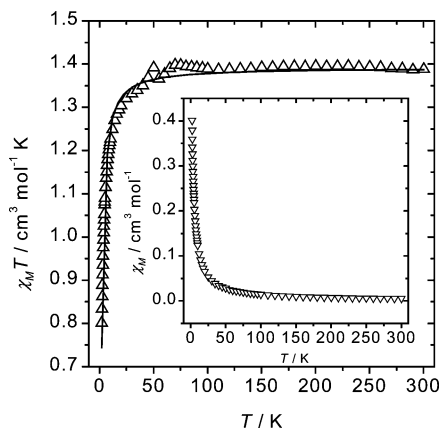


Figure 5. Plots of the  $\chi_M$  vs  $T$  and  $M/N\beta$  vs  $H$  (inset) for **2**.

$\pi$ -systems of these ligands are in favor of forming  $\pi$ – $\pi$  stacking interactions that further stabilize the complexes. In the isonicotinate complexes, the carboxylate plane is almost coplanar to the plane of the pyridine ring,<sup>7–10</sup> whereas in complexes **1**–**8**, the carboxylate plane and the aromatic ring are inclined to each other with dihedral angles from 32.0 to 84.7° because of steric hindrance.

**Magnetic Properties.** Variable-temperature magnetic susceptibility measurements have been made for complexes **2**–**7**. The magnetic behavior of **2** is shown in Figure 5 as  $\chi_M$  vs  $T$  and  $M/N\beta$  (reduced magnetization) vs  $H$  at 2 K (Figure 5 inset).  $\chi_M$  starts almost at 0 cm<sup>3</sup> mol<sup>–1</sup> and rises to 0.037 cm<sup>3</sup> mol<sup>–1</sup>, apparently following the Curie law but with very small  $\chi_M$  values. Most indicative is the curve of the reduced magnetization ( $M/N\beta$ ) vs  $H$  at 2 K: the saturation value is 0.11 $N\beta$ , very far from the 2 $N\beta$  value for two electrons in a dimer of Cu<sup>II</sup>. However, looking at the shape of this curve (similar to a Brillouin curve), we cannot attribute the shape to an antiferromagnetic character of this complex, because this AF character should give a different shape (slope in the reverse sense). Thus, these two features seem to indicate very strong antiferromagnetic coupling between the two Cu<sup>II</sup> ions, with only the impurities (usually monomeric Cu<sup>II</sup> ions) visible. It is well-known that the carboxylato bridge in a syn–syn conformation is able to mediate very strong antiferromagnetic interactions in Cu<sup>II</sup> complexes, with the most common value observed being about –300 cm<sup>–1</sup>.<sup>16–18</sup> Theoretical analysis of this kind of binuclear syn–syn Cu<sup>II</sup> complexes was recently reported.<sup>19</sup> In general, the two most important features are the Cu–Cu distance and the square pyramidal character of the Cu<sup>II</sup> ions. In **2**, this distance is 2.649 Å, and the parameter that indicates the deviation of the square pyramidal geometry ( $\tau = 0$  for regular square pyramidal and  $\tau = 1$  for regular bpt geometry) is 0.006 (thus, close to 0). Both features (Cu–Cu distance

- (16) Dalai, S.; Mukherjee, P. S.; Zangrando, E.; Lloret, F.; Chaudhuri, N. R. *J. Chem. Soc., Dalton Trans.* **2002**, 822 and references therein.  
 (17) Muto, Y.; Nakashima, M.; Tokii, T.; Suzuki, I.; Ohba, S.; Steward, O. W.; Kato, M. *Bull. Chem. Soc. Jpn.* **2002**, 75, 511 and references therein.  
 (18) Steward, O. W.; McAfee, R. C.; Chang, S. C.; Piskor, S. R.; Schreiber, W. J.; Jury, C. F.; Taylor, C. E.; Pletcher, J. F.; Chen, C. S. *Inorg. Chem.* **1986**, 25, 771.  
 (19) Rodríguez-Fortea, A.; Alemany, P.; Alvarez, S.; Ruiz, E. *Chem.–Eur. J.* **2001**, 7, 627.



**Figure 6.**  $\chi_M T$  and  $\chi_M$  (inset) vs  $T$  plots for **3**. Open points are the experimental data, and the solid line represents the best fit obtained from the Hamiltonian given in the text.

and  $\tau$  parameter close to 0) are typical for a strong  $J$  parameter. In **2**, the magnetic data seem to indicate that the  $J$  value has to be on the same order of magnitude as those values reported for the most strongly coupled syn–syn carboxylato systems, like the silane–carboxylato systems ( $J < -500 \text{ cm}^{-1}$ ).<sup>17–19</sup>

For **3**, the susceptibility curve (Figure 6) shows that the  $\chi_M T$  values start at  $1.4 \text{ cm}^3 \text{ mol}^{-1} \text{ K}$ , which is the value corresponding to three isolated  $\text{Cu}^{\text{II}}$  ions (with  $g > 2.00$ ). This value remains constant to 50 K, and then decreases rapidly to  $0.8 \text{ cm}^3 \text{ mol}^{-1} \text{ K}$  at 2 K. This behavior is typical for a weak antiferromagnetic coupling between  $\text{Cu}^{\text{II}}$  ions. The fit of experimental data has been made using the formula given in the literature for a linear trinuclear  $\text{Cu}^{\text{II}}$  system.<sup>20</sup> The Hamiltonian employed was  $H = -J(S_1 S_2 + S_2 S_3)$ . Taking into account the perfect symmetry of the complex, we can take the coupling between  $\text{Cu}(1)\text{--Cu}(2)$  and  $\text{Cu}(2)\text{--Cu}(3)$  to be identical and the coupling between terminal  $\text{Cu}^{\text{II}}$  ions  $\text{Cu}(1)\text{--Cu}(3)$  to be zero. With this hypothesis, the best-fit parameters were  $J = -2.05 \pm 0.02 \text{ cm}^{-1}$ ,  $g = 2.22 \pm 0.002$ , and  $R = 3.3 \times 10^{-4}$  ( $R$  is the agreement factor defined as  $\sum_i [(\chi_M T)_{\text{obs}} - (\chi_M T)_{\text{calc}}]^2 / \sum_i [(\chi_M T)_{\text{obs}}]^2$  (Figure 6)). The most striking feature of this complex is the small  $J$  value, taking into account that the carboxylato bridging ligand in syn–syn conformation gives strong antiferromagnetic coupling.<sup>19</sup> But there are two peculiar aspects in this structure that are very far from the well-known and typical  $[\text{Cu}_2(\text{carboxylato})_4]$ . The  $\text{Cu}\text{--Cu}$  distance is very long,  $4.227 \text{ \AA}$ , and the  $\text{Cu}\text{--O}\text{--O}\text{--Cu}$  dihedral is  $35.8^\circ$ , far from the theoretical value of  $0^\circ$ . Thus, the long  $\text{Cu}\text{--Cu}$  distance and the long dihedral distortion can explain the atypical very small antiferromagnetic coupling.

The  $\chi_M T$  and  $\chi_M$  (inset) vs  $T$  plots for **4** are given in Figure 7.  $\chi_M T$  values start at ca.  $13 \text{ cm}^3 \text{ mol}^{-1} \text{ K}$ , which is the value corresponding to three isolated  $\text{Mn}^{\text{II}}$  ions (with  $g \approx 2.00$ ). This value decreases smoothly to  $4 \text{ cm}^3 \text{ mol}^{-1} \text{ K}$  at 2 K. This behavior is typical for a weak antiferromagnetic coupling between  $\text{Mn}^{\text{II}}$  ions. The magnetism of this kind of trinuclear complex has been exhaustively studied.<sup>21</sup> The fit

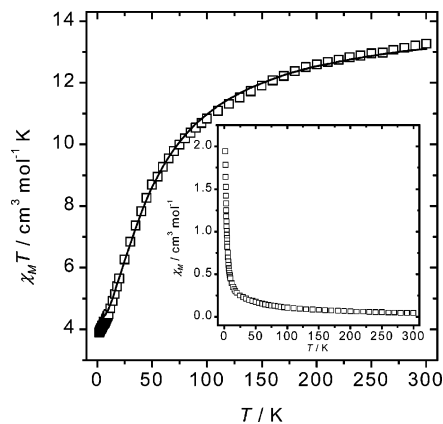


**Figure 7.**  $\chi_M T$  and  $\chi_M$  (inset) vs  $T$  plots for **4**. Open points are the experimental data, and the solid line represents the best fit obtained from the Hamiltonian given in the text.

of experimental data has been made using the expressions given by these authors and by using the Clumag program.<sup>22</sup> The Hamiltonian employed was  $H = -J(S_1 S_2 + S_2 S_3)$ . The best fit parameters were  $J = -3.87 \pm 0.04 \text{ cm}^{-1}$ ,  $g = 2.00 \pm 0.002$ , and  $R = 2.6 \times 10^{-4}$  (Figure 7). The number of trinuclear  $\text{Mn}^{\text{II}}$  complexes with bridging carboxylato groups is limited.<sup>21,23</sup> On the other hand, all but one reported  $[\text{Mn}_3(\text{carboxylato})_6]$  complex present two carboxylato groups in syn–syn conformation, but the third carboxylato bridges two  $\text{Mn}^{\text{II}}$  ions through an oxygen atom from this carboxylato.<sup>23</sup> To the best of our knowledge, only  $[\text{Mn}_3(\text{O}_2\text{CCF}_3)_6(\text{benz})_6]$  ( $\text{benz} = \text{benzotrile}$ ) presents the six carboxylato bridges in syn–syn coordination mode without any isolated oxygen bridging group,<sup>24</sup> such as in **4**. Unfortunately, magnetic data for this last complex have not been reported. It is only possible to compare our magnetic data with those reported in the literature for the complexes described above; in all cases, the  $J$  parameter is small, varying from  $-1.5$  to  $-4.5 \text{ cm}^{-1}$ .<sup>21,23,25</sup> For **4**, the  $J$  value is on the same order of magnitude.

The magnetic properties of **5** in the form of  $\chi_m T$  vs  $T$  plots ( $\chi_m$  is the molar magnetic susceptibility for three  $\text{Co}^{\text{II}}$  ions) are shown in Figure 8. The  $\chi_m T$  value at 300 K is  $11 \text{ cm}^3 \text{ mol}^{-1} \text{ K}$  ( $3.67 \text{ cm}^3 \text{ mol}^{-1} \text{ K}$  for each cobalt ion), which is larger than that expected for the spin-only case ( $\chi_m T = 1.87 \text{ cm}^3 \text{ mol}^{-1} \text{ K}$ ,  $S = 3/2$ ), indicating that an important orbital contribution is involved. The  $\chi_m T$  values continuously decrease from rt to  $2 \text{ cm}^3 \text{ mol}^{-1} \text{ K}$  at 2 K.

The  $\text{Co}^{\text{II}}$  ions are linked by carboxylato groups in syn–syn conformation. As indicated for **3** and **4**, antiferromagnetic

(21) (a) Menage, S.; Vitols, S. E.; Bergerat, P.; Codjovi, E.; Kahn, O.; Girerd, J. J.; Guillot, M.; Solans, X.; Calvet, T. *Inorg. Chem.* **1991**, *30*, 2666. (b) Tangoulis, V.; Malamataris, D. A.; Soulti, K.; Stergiou, V.; Raptopoulou, C. P.; Terzis, A.; Kabanos, T. A.; Kessissoglou, D. P. *Inorg. Chem.* **1996**, *35*, 4974.

(22) The series of calculations were made using the computer program CLUMAG, which uses the irreducible tensor operator (ITO) formalism: Gatteschi, D.; Pardi, L. *Gazz. Chim. Ital.* **1993**, *123*, 231.

(23) Fernández, G.; Corbella, M.; Mahía, J.; Maestro, M. *Eur. J. Inorg. Chem.* **2002**, 2502 and references therein.

(24) Hübner, K.; Roesky, H. W.; Noltemeyer, M.; Bohra, R. *Chem. Ber.* **1991**, *124*, 515.

(25) Rardin, R. L.; Poganiuch, P.; Bino, A.; Goldberg, D. P.; Tolman, W. B.; Liu, S.; Lippard, S. J. *J. Am. Chem. Soc.* **1992**, *114*, 5240. (b) Zhong, Z. J.; You, X. Z.; Mak, T. C. W. *Polyhedron* **1994**, *13*, 2157.

(20) Kahn, O. *Molecular Magnetism*; VCH Publishers: New York, 1993.



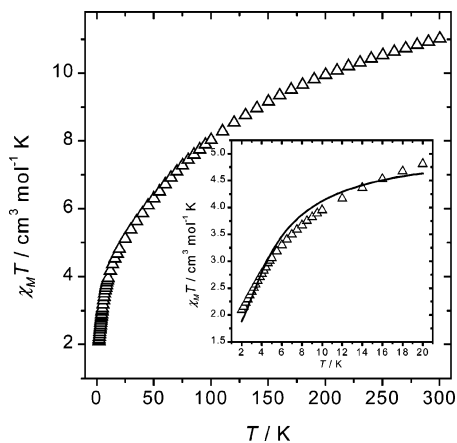


**Figure 8.**  $\chi_M T$  vs  $T$  plot for **5**. In the inset is shown the low-temperature region. Open points are the experimental data, and the solid line represents the best fit obtained from the Hamiltonian given in the text.

interactions are observed in these carboxylate-bridged complexes when the carboxylate adopts the syn–syn conformation. These interactions are very strong for  $\text{Cu}^{\text{II}}$  complexes,<sup>18</sup> but very few  $\text{Co}^{\text{II}}$  complexes with this interaction have been rigorously studied from a magnetic point of view, as they are always antiferromagnetically coupled.<sup>26</sup>

For the interpretation of the magnetic measurements, we must point out the importance of the spin–orbit coupling of the  $\text{Co}^{\text{II}}$  ions.<sup>27</sup> The degeneracy of the  $^4\text{T}_{1g}$  ground state of the octahedral  $\text{Co}^{\text{II}}$  ion prevents any easy fit, except in the low-temperature region ( $<20$ – $25$  K) in which  $\text{Co}^{\text{II}}$  systems may be described as having an effective spin of  $1/2$  with large anisotropy. Thus, for simple systems, it is possible to fit the data at low temperatures with special computational programs.<sup>28–30</sup> The magnetic data of **5**, from 20 to 2 K (Figure 8 inset), are fitted to a model<sup>28</sup> that considers isotropic exchange interactions between the magnetic  $\text{Co}^{\text{II}}$  ions but anisotropic  $g$  values. In the case of the trimer **5**, the general-exchange Hamiltonian that describes the exchange interactions between the effective  $S = 1/2$  spins may be written as

$$H = -2 \sum_{i=x,y,z} J_{1i} (S_{1i} S_{2i} + S_{2i} S_{3i})$$

In this Hamiltonian, the coupling ( $J_{13}$ ) between the two terminal  $\text{Co}^{\text{II}}$  ions is assumed to be nil. Assuming that the  $g$

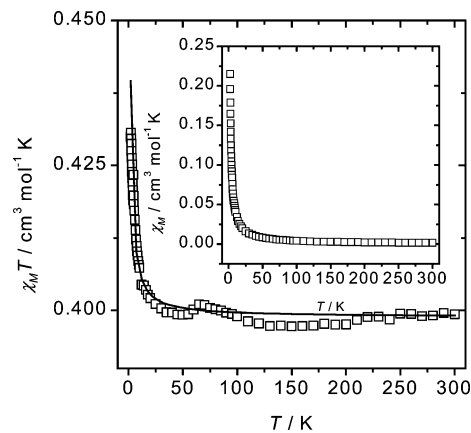


**Figure 9.**  $\chi_M T$  and  $\chi_M$  (inset) vs  $T$  plots for **6**. Open points are the experimental data, and the solid line represents the best fit obtained from the formula given in the text.

parameters are equivalent, the exchange parameters  $J = -2.0 \text{ cm}^{-1}$ ,  $g_{\perp} = 5.0$ , and  $g_{\parallel} = 2.2$  provide an excellent description of the magnetic susceptibility (Figure 8 inset). The found  $g$  values are very reasonable values for  $\text{Co}^{\text{II}}$  sites with octahedral coordination.<sup>31</sup>

The  $\chi_M T$  and  $\chi_M$  (inset) vs  $T$  plots for **6** are given in Figure 9 for one  $\text{Cu}^{\text{II}}$  ion.  $\chi_M T$  values start at  $0.4 \text{ cm}^3 \text{ mol}^{-1} \text{ K}$ , which is the value corresponding to one isolated  $\text{Cu}^{\text{II}}$  ion (with  $g \approx 2.00$ ). This value is constant to approximately 50 K and then slightly increases to close to  $0.43 \text{ cm}^3 \text{ mol}^{-1} \text{ K}$  at 2 K. This behavior is typical for a very weak ferromagnetic coupling between  $\text{Cu}^{\text{II}}$  ions in the layer. The magnetism of this kind of 2D  $\text{Cu}^{\text{II}}$  system has been theoretically studied by several authors, such as Lines<sup>32</sup> and Rushbrooke.<sup>33</sup> The best fit parameters, using the more general Rushbrooke formula, were  $J = 0.07 \pm 0.001 \text{ cm}^{-1}$ ,  $g = 2.06 \pm 0.001$ , and  $R = 5.3 \times 10^{-6}$  (Figure 9). In the structure,  $\text{Cu}^{\text{II}}$  ions are bridged by the ligand through the nitrogen atoms and one of the oxygens of the carboxylate group in equatorial–equatorial positions. The  $\text{Cu}^{\text{II}}$ – $\text{Cu}^{\text{II}}$  distance is  $8.717 \text{ \AA}$ , which is indicative of the small coupling. The ferromagnetic character (even very small but not nil) is an open question. No easy explanation can be given for this feature.

The magnetic properties of **7** are shown in the form of  $\chi_M$  and  $\chi_M T$  (inset) vs  $T$  plots (Figure 10) for one  $\text{Mn}^{\text{II}}$  ion. The  $\chi_M T$  values start at  $4.3 \text{ cm}^3 \text{ mol}^{-1} \text{ K}$ , which is the value corresponding to one isolated  $\text{Mn}^{\text{II}}$  ion (with  $g \approx 2.00$ ). This value decreases smoothly to close to  $0 \text{ cm}^3 \text{ mol}^{-1} \text{ K}$  at 2 K. This behavior is typical for a weak antiferromagnetic coupling between  $\text{Mn}^{\text{II}}$  ions in the chain. The magnetism of this kind of 1D  $\text{Mn}^{\text{II}}$  system has been theoretically studied by several authors, such as Wagner et al.<sup>34</sup> and, mainly, Fisher.<sup>35</sup> Fisher's treatment allows one to analyze the

- (26) Little, I. R.; Straughan, B. P.; Thornton, P. *J. Chem. Soc., Dalton Trans.* **1986**, 2211.  
 (27) Mabbs, F. E.; Martin, D. J. *Magnetism and Transition Metal Complexes*; Chapman and Hall: London, 1973.  
 (28) MAGPACK program: (a) Borrás-Almenar, J. J.; Clemente-Juan, J. M.; Coronado, E.; Tsukerblat, B. S. *Inorg. Chem.* **1999**, *38*, 6081. (b) Borrás-Almenar, J. J.; Clemente-Juan, J. M.; Coronado, E.; Tsukerblat, B. S. *J. Comput. Chem.* **2001**, *22*, 985.  
 (29) Caneschi, A.; Dei, A.; Gatteschi, D.; Tangoulis, V. *Inorg. Chem.* **2002**, *41*, 3508.  
 (30) Clemente, J. M.; Andres, H.; Aebersold, M.; Borrás-Almenar, J. J.; Coronado, E.; Güdel, H. U.; Büttner, H.; Kearly, G. *Inorg. Chem.* **1997**, *36*, 2244. (b) Andres, H.; Aebersold, M.; Güdel, H. U.; Clemente, J. M.; Coronado, E.; Büttner, H.; Kearly, G.; Zolliker, M. *Chem. Phys. Lett.* **1998**, *289*, 224. (c) Andres, H.; Clemente-Juan, J. M.; Aebersold, M.; Güdel, H. U.; Coronado, E.; Büttner, H.; Kearly, G.; Melerio, J.; Burriel, R. *J. Am. Chem. Soc.* **1999**, *121*, 10028. (d) Andres, H.; Clemente-Juan, J. M.; Basler, R.; Aebersold, M.; Güdel, H. U.; Borrás-Almenar, J. J.; Gaita, A.; Coronado, E.; Büttner, H.; Janssen, S. *Inorg. Chem.* **2001**, *40*, 1943.

- (31) Carlin, R. L. *Magnetochemistry*; Springer: Berlin, 1986.  
 (32) Lines, M. E. *J. Phys. Chem. Solids* **1970**, *31*, 101.  
 (33) (a) Rushbrooke, G. S.; Wood, P. *J. Mol. Phys.* **1963**, *6*, 409. (b) de Muro, I. G.; Mautner, F. A.; Insausti, M.; Lezama, L.; Arriortua, M. I.; Rojo, T. *Inorg. Chem.* **1998**, *37*, 3243.  
 (34) Wagner, G. R.; Friedberg, S. A. *Phys. Lett.* **1964**, *9*, 11.  
 (35) Fisher, M. E. *Am. J. Phys.* **1964**, *32*, 343. (b) Escuer, A.; Mautner, F. A.; Sanz, N.; Vicente, R. *Inorg. Chem.* **2000**, *39*, 1668.

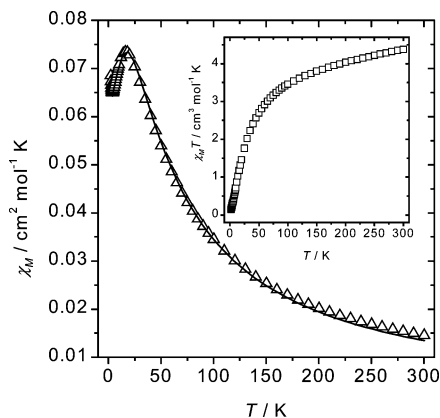


**Figure 10.**  $\chi_M$  and  $\chi_M T$  (inset) vs  $T$  plots for **7**. Open points are the experimental data, and the solid line represents the best fit obtained from the formula indicated in the text.

magnetic data by means of an analytical expression assuming an infinite number of classical spins ( $S = 5/2$ ).<sup>35</sup> The Hamiltonian employed was  $H = -\sum J_{ij} S_i S_j$ . The best fit parameters were  $J = -2.85 \pm 0.01 \text{ cm}^{-1}$ ,  $g = 2.00 \pm 0.004$ , and  $R = 2.6 \times 10^{-7}$  (Figure 10). In the fit, the last  $\chi_M T$  points (with a tendency to increase) have been omitted, because they can indicate some small percentage of paramagnetic impurities. The number of 1D  $\text{Mn}^{\text{II}}$  complexes with bridging carboxylate groups is rather limited. Magnetic parameters indicate weak antiferromagnetic coupling in all of them.<sup>36</sup>

In conclusion, we have obtained a series of new complexes having dimeric and trimeric structures and 1D, 2D, and 3D frameworks of 9-acridinecarboxylate and 4-quinolinecarboxylate ligands. An ordinary comparison of structures with related ligand complexes has been performed, and shows that the coordination geometry of center metal ions, the ligands' bulky bodies, and the tendency to form  $\pi$ - $\pi$  stacking are important factors in influencing the structures of their complexes. The magnetic properties for **2–7** have been investigated, along with the corresponding  $J$  parameter related to their structural characteristics.

**Acknowledgment.** This work was supported by the National Science Funds for Distinguished Young Scholars of China (20225101) and NSFC (20373028), by a Grant-In-Aid for Science Research in a Priority Area "Metal-Assembled Complexes" (401-10149106) from the Ministry of Education, Science, Sports, and Culture, Japan, and by the Spanish government (Grant BQU2003-00539).

**Supporting Information Available:** Figures S1–S4: hydrogen bonding interactions, 3D structures, etc., of the various compounds. This material is available free of charge via the Internet at <http://pubs.acs.org>.

IC050886D

(36) (a) Cano, J.; De Munno, G.; Sanz, J.; Ruiz, R.; Lloret, F.; Faus, J.; Julve, M. J. *Chem. Soc., Dalton Trans.* **1994**, 3465. (b) Chen, X. M.; Mak, T. C. W. *Inorg. Chim. Acta* **1991**, 189, 3.